

Carbon Nanotube Based High Performance Biosensing Platform

Subjects: Biotechnology & Applied Microbiology

Contributor: Jagannath Mondal, Jeong Man An, Sachin S. Surwase, Kushal Chakraborty, Sabuj Chandra Sutradhar, Joon Hwang, Jaewook Lee, Yong-Kyu Lee

After the COVID-19 pandemic, the development of an accurate diagnosis and monitoring of diseases became a more important issue. In order to fabricate high-performance and sensitive biosensors, many researchers and scientists have used many kinds of nanomaterials such as metal nanoparticles (NPs), metal oxide NPs, quantum dots (QDs), and carbon nanomaterials including graphene and carbon nanotubes (CNTs). Among them, CNTs have been considered important biosensing channel candidates due to their excellent physical properties such as high electrical conductivity, strong mechanical properties, plasmonic properties, and so on.

Keywords: carbon nanotubes ; high-performance biosensors ; nanomaterials-based biosensors

1. Introduction

The detection of biological components is important in several areas ranging from healthcare, clinical medicine, environmental control, and food processing to homeland security ^{[1][2]}. Therefore, the development of reliable and cost-effective devices is highly demandable for our healthy lifestyles ^[3]. Sensor a class of devices that has been explored to detect a range of gas molecules to biomolecules. Biosensors are analytical devices that can combine biomolecules recognition via chemical or physical transduction ^[4]. Biosensor development is being driven increasingly by nanotechnology. Signal transduction is the basis for the operation of biosensors ^[5]. There are three elements in this system: a bio-recognition element, a bio-transducer, and an electronic system consisting of a display, a processor, and an amplifier. It interacts with a specific analyte through its bio-recognition element ^[6]. A wide range of samples can be tested with biosensors, including body fluids, food samples, and cell cultures. The main features of biosensors include: (a) being highly specific for the analyte, (b) reaction must be unaffected by factors like pH, temperature, or stirring, and (c) the linearity of the response will be maintained over a certain range of analyte concentrations ^{[7][8][9]}.

One of the most widely used nanomaterials over the last two decades is carbon nanotubes (CNTs). This highly active field of research has a wide variety of CNT forms, and new forms are being designed and fabricated on a continuous basis. Hence, CNTs are receiving considerable attention in many fields of application from medicine ^[10], agriculture ^[11], and food safety ^[12] to bioprocessing ^[13], environmental ^[14], and industrial monitoring ^[15]. In recent years, CNTs have drawn interest in biosensor devices due to their several unique properties ^{[16][17][18][19]}. Specifically, CNTs possess a wide surface area and extensive free surface energy, and can easily stabilize the biomolecules at the biosensor surface through strong adsorb capability ^{[20][21][22]}. The strong carbon-carbon bonds and nanostructure of chemically modified carbon nanotubes (CNTs) are attributed to their outstanding electric conductivity, exceptional tensile strength, thermal conductivity, and optical properties allowing them to efficiently transmit signals associated with detecting analytes, metabolites, or disease biomarkers ^{[23][24]}. The use of CNTs for biomedical applications has therefore attracted considerable attention. Owing to their high surface-to-volume ratio, CNTs are capable of detecting biological components at ultra-fast speed with minimal concentrations. With the great advantages of CNTs-based biosensors such as high sensitivity, fast response time, lower potential for redox reactions, and longer lifetime with stability compared to other sensors based on metal oxides, or silicon-based materials ^{[25][26]}. These potential characteristics of CNTs have shed to elevate the research interests towards the development of biosensors. Electrochemical sensors and optical sensors made from CNTs have been developed for several applications, including the detection of heavy metals ^[27], in addition to field-effect devices for detecting virus infection ^[28], bacteria ^[29], cancer ^{[30][31]}, diabetes ^[32], and biological components detection ^[33].

The entry is an overview of carbon nanotubes (CNTs) and their derivatives as high-performance biosensors. The preparative methods such as electric-arc discharge, laser ablation, and chemical vapor deposition (CVD) of the CNTs have been described briefly here. The efforts made on the toxicology profile and mechanism of sensing of CNTs in this

entry. Later, researchers have illustrated insightfully the applications of CNTs as a biosensor for the detection of cancer and diabetes, biological components such as carbohydrates, proteins, essential elements, some bacteria, and viruses (**Figure 1**). Additionally, the recent development towards the commercialization of CNTs and their derivatives sensors has been discussed.

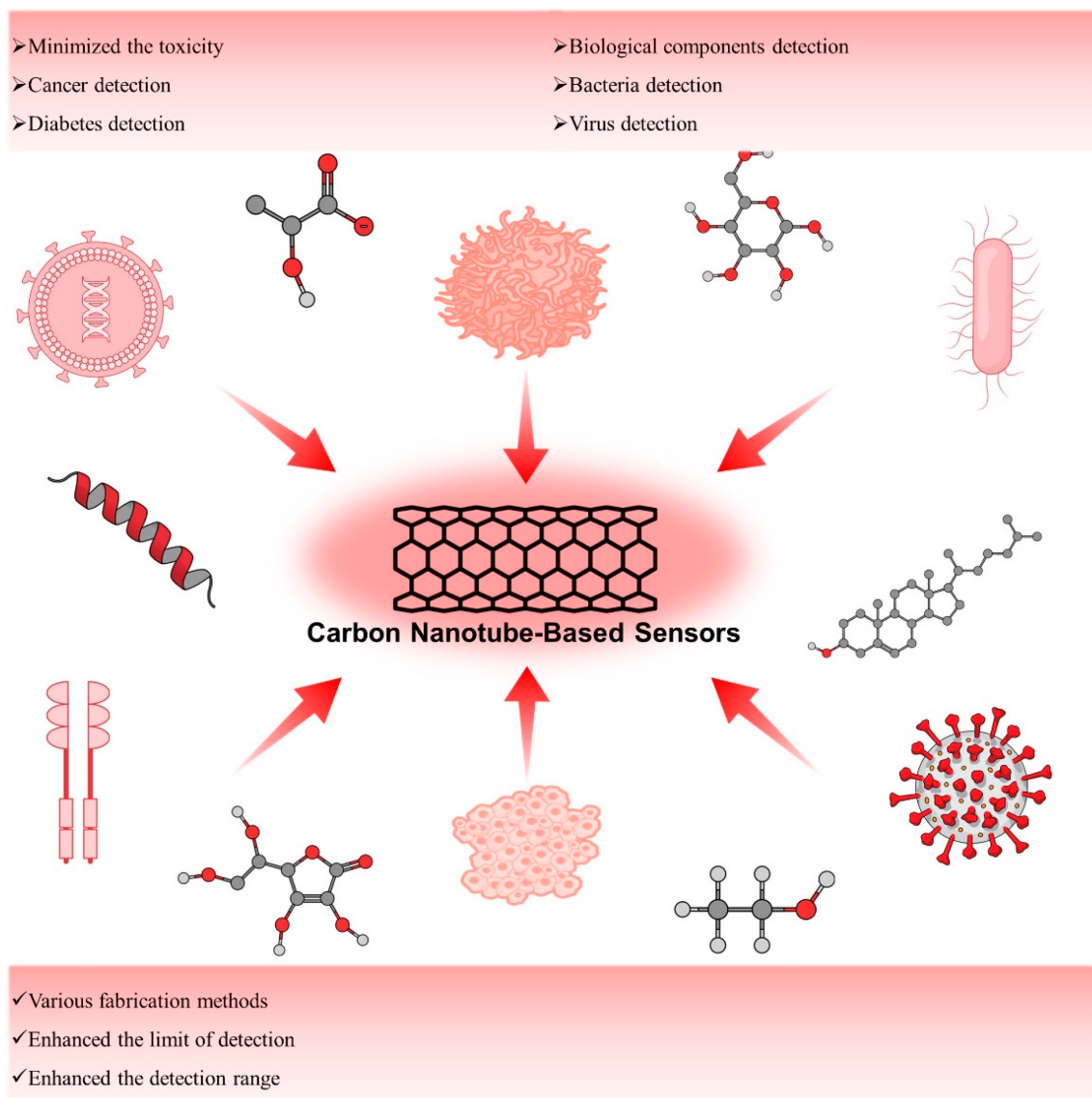


Figure 1. Schematic presentation of CNT-based biosensors.

2. Preparation of Carbon Nanotubes (CNTs)

After the discovery of synthetic pathways of C_{60} and other types of fullerenes [34], it ignited the interest among synthetic chemists for other carbon-based materials with different structural possibilities. The first multi-walled CNT (MWCNT) synthesis in the laboratory was reported by Sumio Iijima in 1991 by using carbon black and graphite as precursor materials in a regulated environment. He named it "Helical microtubules" [35]. Iijima used the arc-discharge evaporation method to produce needle-like structures (ranging from 4–30 nm in length and up to 1 μ m in diameter) comprising coaxial tubes of graphite sheets, but his unquenchable reaction setting was also associated with some major drawbacks including uneven shape, size, and mechanical strength as well as purity, which are the most important parameters associated with their applicability. In the case of single-walled CNT (SWCNT), it was jointly discovered by Iijima and Ichihashi [36] and Bethune and colleagues [37] in 1993. They used arc discharge methods to produce CNTs whereas the former group used an iron catalyst and the latter one used a cobalt catalyst. In both cases, uneven size was the biggest issue as Iijima and Ichihashi reported a diameter between 0.75 and 13 nm whereas Bethune and colleagues reported a diameter between 1.2 and 20 nm.

Thirty years after the first encounter, there is revolutionary progress in the field of CNTs. Currently, a variety of synthetic techniques are being employed with modified approaches and tweaks to produce CNTs with some exceptional features due to the recent revelation of CNT application in the pharmaceutical division.

Electric-arc discharge, laser ablation, and chemical vapor deposition (CVD) are commonly used to produce several types of CNTs.

2.1. Electric-Arc Discharge

The oldest method of synthesis of CNTs is the arc discharge method. It utilizes the principle of breaking down the gas to generate plasma. The main component of this experimental setup is two parallelly attached electrodes (either horizontally or vertically) where the anode is crammed up with carbon precursors along with catalysts whereas the cathode is a pure graphite rod. The chamber is filled with an inert gas or engulfed inside a liquid atmosphere. Both AC and DC power supplies can be used in this system whilst the electrodes are kept in close contact (1–2 mm) to generate an arc and attain a steady discharge. Plasma is generated by arc current at an extremely elevated temperature (4000–6000 K) which sublimates the carbon precursor in the anode. The carbon vapors accumulate in the gaseous phase and get deposited at the cathode due to the temperature gradient. After cooling down it is taken out and purified for further investigation and examined under an electron microscope for further assessment of the morphology [38].

CNTs grow in different phases in this method as in the vapor phase, liquid phase, solid phase, and crystal phase, respectively [39][40][41][42].

In the arc discharge method, CNTs get synthesized by sublimation of a carbon precursor. Carbon black [43][44][45][46] and graphite [47][48][49][50][51][52][53][54][55][56] are commonly used in this scenario although some other carbon precursors namely fullerene waste soot [57], polyvinylalcohol [58], and other hydrocarbons including toluene, xylene, cyclohexane, cyclohexanone, n-hexane, n-heptane, n-octane, and n-pentane [59] are also reported. Some important parameters namely, the pressure of the inert gas, optimal voltage as well as the choice of the catalysts are critical for synthesizing highly pure CNTs via this method. For example, one of the recent findings suggests that the Co-MCM-41 catalyst helps to produce CNTs with large diameter distribution along with bulk production [60].

2.2. Laser Ablation

Laser vaporization or the laser ablation method is one of the most efficient methods to synthesize CNTs. It uses the same principle of arc discharge method as vaporization of carbon precursors in a laser-assisted pathway followed by depositing on the substrate. In 1995, R.E. Smalley and colleagues reported the first SWCNT synthesis by directly vaporizing transition metal/graphite composite rods in a laser-aided pathway. The experimental setup consists of a furnace, a quartz tube with a window, a target carbon composite doped with catalytic metals, a water-cooled trap, and flow systems for the buffer gas to maintain constant pressures and flow rates along with a pressure gas flow controller. Typically, an Nd:YAG (neodymium-yttrium-aluminum-garnet) laser or a CO₂ laser is introduced through the window and focused onto the target. The target gets vaporized at a controlled pressure. The buffer gas transports the manufactured SWNTs towards the water-cooled trap, where they are collected [61]. In this method, it is possible to get a yield up to 90% but the high cost makes it pretty tough to implement in large-scale production.

Arc discharge and laser ablation are both energy-intensive processes, therefore comparisons between them revealed some noteworthy commonalities. Such a situation is exceedingly uneconomical for performance at an industrial level. Both techniques have extremely rigorous purification protocols and huge graphite requirements as a target material, which restricts their use in large-scale industrial manufacturing.

2.3. Chemical Vapor Deposition (CVD)

The thermal CVD method is one of the simplest and most cost-efficient methods in the field of CNT synthesis which can produce a high amount of yield. CVD synthesized CNT was reported as defective at the beginning, but since 1998, after recognizing its potential, a significant number of changes have been incorporated and nowadays it is one of the most widely used methods for synthesizing CNTs. Currently, it is possible to engineer high-quality SWCNTs and MWCNTs via this method. One of the most important advantages it has over arc discharge and laser ablation methods is the temperature region as it can be operated in lower regions such as 550–1000 °C. First, the carbon source gas and the carrier gas are introduced into the reaction chamber while the temperature is between 550 and 1000 °C. Next, the gas is decomposed to produce carbon atoms on a coated catalyst substrate while the temperature is kept at a high temperature and finally carbon nanotubes are produced. The most common transition metal catalysts are cobalt (Co) [62], iron (Fe), nickel (Ni), copper (Cu), chromium (Mo), and their alloys [63]. In most cases, carbon gases such as methane, ethanol, ethylene, acetylene, and benzene are used as the source of carbon [64][65][66].

2.4. Others

Apart from conventional methods, there are also some other methods emerging for CNT synthesis, namely solvothermal [67], low-temperature plasma reduction [67], sol-gel [68], and flame [69] but low yield and difficult parameter control make it very hard for them to get used in frontline synthesis.

3. Applications of Carbon Nanotubes as Biosensors

3.1. Carbon Nanotube-Based Sensors for Detection of Cancer

3.1.1. CD44 Expressing Cancer Cell

Recently, cancer stem cells (CSCs) were identified as rare tumor-initiating cell populations which show self-renewal, pluripotent, and highly tumorigenic which makes them more resistant to breast cancer treatment. These cells are mainly responsible for breast cancer recurrence since even though most of the cells were killed by therapy, still few CSCs can regenerate tumors. Notably, CSCs are isolated from various cancer types including breast, brain, lung, colon, and skin cancer or melanoma. In particular, the case of breast cancer CSCs is identified by the presence of characteristic biomarkers namely CD44 and CD24 as well as one of the enzyme activities (ALDH1). This literature suggests that it is very important to detect and target the CSCs and their daughter cells responsible for cancer regeneration to achieve double remission.

3.1.2. EpCAM Expressing Cancer Cell

Epithelial cell adhesion/activating molecule abbreviated as EpCAM is the first tumor-associated antigen and currently it is considered as the most intensely and frequently expressed tumor-associated antigen. It is found to be expressed in a great variety of cancer types and it can be utilized as a biosensor application. Circulating tumor cells (CTCs) can also express EpCAM antigen and a nanoprobe or sensor can be developed to study the presence of these biomarkers on cancer cells by using anti-EpCAM antibody. Neoh et al. developed a CNT chip containing promising microfluidic technology for the effective capture and release of the CTCs. This technique allowed to perform downstream analysis of CTCs such as molecular and functional analyses. Researchers successfully developed a chip platform with the ability to not only capture the CTCs but also release them in a pH-responsive manner with higher sensitivity. This platform was tested for the clinical samples for the optimization of a device in order to maximize the cell capture and release efficiency, viability as well as application of this technology for single-cell molecular profiling and in vitro culture. Since EpCAM is a widely expressed antigen by various cancer cells, this platform could be generalized for different types of CTCs capture and detailed analysis.

3.1.3. CA19-9 Expressing Cancer Cell

Carbohydrate antigen 19-9 (CA 19-9) is a cell protein glycoprotein also known as Sialyl Lewis-a produced by ductal cells in the pancreas, salivary gland, biliary system, and epithelial cells in the stomach and colon. It is the most used biomarker for the diagnosis and management of prognosticating pancreatic ductal adenocarcinoma (PDAC) [70]. Its widespread expression in several tumor cells makes it useful for the diagnosis of other tumor types apart from its historical use in the case of PDAC. Considering its diagnostic potential Thapa et al. developed a highly sensitive biosensor to detect the pancreatic cancer biomarker CA19-9. This developed biosensor based on nanomaterials promises cheaper, faster, and more efficient early diagnosis of pancreatic cancer as compared to traditional bulky devices. To fabricate the device, MWCNTs with functionalized anti-CA19-9 antibody were utilized.

3.1.4. VEGF Expressing Cancer Cell

Vascular endothelial growth factor (VEGF) is considered a main angiogenic factor in the case of many malignant tumors. VEGF acts by specific effects by stimulating cell growth and migration as well as increasing vascular permeability. It is a promising biomarker, especially in the case of the prognosis of cancer cells [71]. Electrochemical aptasensors are promising agents due to their advantages of being cheaper and the possibility to have quantitative analysis.

3.2. Carbon Nanotube-Based Sensors for Detection of Diabetes

Two primary approaches are used while incorporating nanotechnology for glucose sensing applications. In the first approach, sensors can be designed by using micro or macroscopic components while incorporating nanomaterials in the sensing device. These nanomaterials in the sensor design offer several advantages such as higher surface area and enhanced catalytic activity. In the case of the second approach, nanofabrication can generate nanoscale sensors for glucose sensing. These sensors have some advantages such as offering continuous monitoring and avoiding foreign body

responses of the immune system resulting in a longer life as compared to traditional sensors. In the case of diabetes, CNTs incorporation is heavily investigated as enzymatic electrode detection of glucose due to the electron transfer ability of the CNT and their surface areas [72]. CNT-based electrochemical biosensors immensely helped with glucose sensing. Both single-walled CNTs as well as multi-walled CNTs have been explored as a nanomaterial for the detection of glucose. Functionalization of MWCNTs is less complex as compared to the SWCNTs since GOx could be directly adsorbed on the surface of MWCNTs as compared to the SWCNTs where a covalent linkage is required. It is possible to fabricate the best-performing glucose sensing devices when they are combined with the other nanomaterials [73].

Enzymatic sensors are based on the use of enzymes for the conversion of an electro-inactive substrate into an electro-active product such as the use of glucose oxidase enzyme on a platinum electrode. On the other hand, non-enzymatic glucose sensors are based on the direct electrochemical oxidation of glucose. Most of the researchers focused on the development of enzymatic electrochemical sensors using glucose oxidase, but recently, non-enzymatic sensors using direct electrochemistry of glucose on noble metals are coming forward as next-generation glucose sensing technology [74]. Here are examples of enzymatic and non-enzymatic sensors fabricated to enhance the ultrasensitive detection of glucose. Researchers tried to use carbon nanotubes to either modify the sensitivity of enzyme-based sensors that are prone to temperature-based degradation or used an alternative non-enzymatic sensing strategy by combining the carbon nanotubes in the device fabrications. Additionally, researchers have presented a tabular form of CNT-based enzymatic and non-enzymatic biosensors (**Table 1**).

Table 1. Summarization of CNT-based enzymatic and non-enzymatic biosensors.

Methods	Analytes	Limit of Detection	Detection Range	Ref.
Enzymatic	Lactate	Not reported	5–20 nM	[75]
	Uric acid	9.91 μ M	50 to 650 μ M	[76]
	Glucose	0.58 μ M	0.8 to 250 μ M	[77]
	Glucose	3×10^{-4} M	$(1-15) \times 10^{-3}$ M	[78]
	Glucose	5×10^{-5} M	$(0-5) \times 10^{-3}$ M	[79]
	Glucose	2.99×10^{-6} M	$(3-14) \times 10^{-3}$ M	[80]
	Ethanol	1×10^{-5} M	$(1-5) \times 10^{-4}$ M	[81]
	Urease	67 μ M	1.0–25.0 mM	[82]
	Alcohol dehydrogenase	10 μ M	0.1 to 0.5 μ M	[78]
	Choline	0.6 μ M	3–120 μ M	[83]

Methods	Analytes	Limit of Detection	Detection Range	Ref.
Non-enzymatic	Pyruvic acid	0.048 μM	0.1–200 μM	[84]
	Human epidermal growth factor receptor 2	7400 pg/mL	10–110 ng mL^{-1}	[85]
	Cholesterol	0.5 nM	0.001–3 μM	[86]
	glucose	500 nM	2–19,600 μM	[87]
	Zearalenone	0.15 pg mL^{-1}	0.001–0.1	[88]
	Long non-coding RNAs	42.8 fM	10^{-14} – 10^{-7} M	[89]
	MicroRNA 21	0.01 fM	10^{-17} – 10^{-6} M	[90]
	Thrombin	0.08 pM	0.001–4 nM	[91]
	Human epidermal growth factor receptor 2	50 fg mL^{-1}	0.1 pg mL^{-1} –1 ng mL^{-1}	[92]
	Cardiac troponin T	0.04 pg mL^{-1}	0.1–8 pg mL^{-1}	[93]
	Urea	4.7 nM	0.066–20,600 μM	[94]
	Ascorbic acid	0.85 nM	0.001–8000 μM	[95]
	Glucose	645 nM	20–10,500 μM	[96]
	Glucose	0.33 nM	10–2000 μM	[97]
	Dopamine	9.5 nM	0.033–1 μM	[98]
	Potassium ions	Not reported	1000–32,000 μM	[99]
	Hydrogen peroxide	Not Reported	5×10^{-6} – 5×10^{-3} M	[100]
	MicroRNA 155	3.34×10^{-14} M	1×10^{-13} – 1×10^{-9} M	[101]
	Digoxin	7.95×10^{-12} M	2.65×10^{-11} – 6.8×10^{-10} M	[102]
	Sequence specific to chronic myelogenous leukemia	1 fM	10^{-15} – 10^{-6} M	[103]
	Myeloperoxidase	327 ng mL^{-1}	Not reported	[104]
	SARS-CoV-2 spike protein	35 mg L^{-1}	Not reported	[105]
	SARS-CoV-2 spike protein	0.55 fg mL^{-1}	0.0055–5.5 pg mL^{-1}	[106]
	Ascorbic acid	76.5 pM	100 pM to 1 mM	[107]

3.3. Carbon Nanotube for Biological Components Detection

The detection of biological components is very important in biology, clinical science, and in hospitals facing real patients. In particular, it can make an early diagnosis of the disease, thereby allowing the patient to receive a faster and more correct response to the disease [108]. This is closely related to the quality of life of patients. However, even if the patient has a specific disease, if the biological component cannot be detected or not, the patient's life will be very difficult and painful, the treatment cost will increase significantly, and a cure cannot be guaranteed. In fact, many patients around the world suffer from misdiagnosis and late diagnosis [109]. In order to fundamentally solve these problems, it is urgent and very important to develop materials, devices, and equipment that can detect biological components with high performance and high sensitivity.

CNTs have also been studied for use in the detection of biological components. CNTs have many advantages in the detection of various components due to their unique physical properties, such as large surface area [110], tubular three-dimensional structure [111], and the possibility of multiple modifications [112]. Here, researchers introduce studies of CNTs for the detection of biological components. Recently, much research has been conducted to develop a sensor that detects glucose using CNTs. The detection of glucose in the serum is very important to mankind and has been performed for a long time. Measurement of blood glucose levels, especially in diabetic patients, is indispensable that must be performed daily and frequently. Scientific, patient-friendly, and modern blood glucose level measurement began with Clinistix developed by Kohn in 1957 [113], and Dextrostix developed by Ernie Adams in 1965 [114]. In a recent glucose detection

study, a biosensor using ZnFe_2O_4 , CNT, and glucose oxidase was developed [77]. Briefly, ZnFe_2O_4 was conjugated with CNT by a one-step solvothermal approach using acid-treated CNT as a precursor. Glucose oxidase (GOD) was linked to ZnFe_2O_4 -conjugated CNT by coupling reaction between the amine group and carboxyl group (ZnFe_2O_4 -CNT-GOD). When glucose is added to ZnFe_2O_4 -CNT-GOD, glucose is oxidized by GOD. In this process, the intermediate product, hydrogen peroxide, oxidizes the 3,3',5,5'-tetramethylbenzidine (TMB) substrate and is eventually visualized in blue. In this process, ZnFe_2O_4 acts as a peroxidase and not only accelerates the overall reaction but also increases the intensity of the detected signal.

ZnFe_2O_4 -CNT-GOD has a glucose detection range of 0.8 to 250 μM with a detection limit of 0.58 μM . ZnFe_2O_4 -CNT-GOD did not react with lactose, maltose, fructose, sucrose, uric acid, dopamine, cystine, albumin, and ascorbic acid, so there was no component detection, but only a glucose-specific reaction occurred. In addition, the ZnFe_2O_4 -CNT-GOD showed only a negligible change in the detection sensitivity of glucose even in the presence of 100 μM of copper, zinc, potassium, calcium, and iron ions. The authors report that the fabrication method of ZnFe_2O_4 -CNT-GOD is simple, maintains the sensing activity for at least 20 days, and can be reused at least five times. Wang C et al. reported enzyme-functionalized CNTs and their application in glucose and Fe^{2+} detection [115]. Briefly, CNT was modified with carboxylation for functionalization. Later, carboxylated CNTs were covalently conjugated with GOD and/or horseradish peroxidase (HRP) (CNT-HRP-GOD). CNT-HRP-GOD detects glucose through the chain reaction between glucose, GOD, and HRP. In this process, the intermediate product, hydrogen peroxide, oxidizes the 3,3',5,5'-tetramethylbenzidine (TMB) substrate and results in the production of colorimetric products (blue). Fe^{2+} reacts with hydrogen peroxide and leads to a lower concentration of hydrogen peroxide, which in turn decreases the oxidation state of TMB and eventually causes a lower colorimetric absorbance of the solution. CNT-HRP-GOD has a glucose and Fe^{2+} detection range of 1 to 100 μM with a detection limit of glucose and Fe^{2+} of 0.3 and 0.22 μM , respectively. CNT-HRP-GOD did not react with other sugars except glucose and did not react with albumin and ascorbic acid, so it was verified as a biosensor through a glucose-specific reaction.

Alcohol detection can be applied to a variety of fields, from the quality analysis of bio-alcohol, which has been actively researched and manufactured recently, to checking the blood alcohol concentration and analyzing the quality of alcoholic beverages. Wilson, T et al. reported a CNT-based alcohol biosensor [81]. They modified CNTs using polytyramine (PT) and glassy carbon (GC). PT has been electro-deposited onto MWCNT-modified GC electrodes via oxidation of tyramine (GC/MWCNT/PT). ADH immobilization for alcohol detection was improved by the PT layer. The polymeric film was formed on the electrode surface of MWCNT and it was confirmed using SEM and XPS. In order to detect alcohol with GC/MWCNT/PT, GC/MWCNT/PT was immersed in 0.05 M of sodium phosphate buffer (PBS) which contained 1 mg mL^{-1} of alcohol dehydrogenase (ADH). The EDC/NHS coupling reaction was performed for one hour for the conjugation of the two substances (GC/MWCNT/PT/ADH). This alcohol biosensor showed a sensitivity of $4.28 \pm 0.06 \mu\text{A mM}^{-1} \text{ cm}^{-2}$, a regression coefficient of 0.9993, and a response time of 5 s. Furthermore, it had a 10 μM limit of detection and it almost accurately detected the alcohol content of commercial alcoholic beverages at a level of recovery of 97.4–102.1%.

Ascorbic acid is one of the water-soluble vitamins, and since L-gulonolactone oxidase is not present in the body, ascorbic acid must be consumed as a food or nutritional supplement [116]. A deficiency of this causes scurvy [117]. Ascorbic acid acts as an antioxidant in the body, protecting normal cells from various reactive oxygen species [118] and helping to maintain the immune system [119]. In addition, it suppresses various inflammatory reactions [120] and aging [121], and helps the elderly to maintain cognitive ability and memory, thereby helping to prevent Alzheimer's disease [122]. Zhao, Y et al. reported an ultra-sensitive biosensor for the voltammetric determination of ascorbic acid (AA) [123]. For the fabrication of CNT-based high-sensitivity ascorbic acid sensors, MWCNTs were surface modified with glassy carbon electrodes (GCEs), graphene oxide (GO), and gold nanorods (AuNRs). Since the aggregation of MWCNTs reduces the detection sensitivity of biological components, prevention of aggregation improves the sensitivity. In this study, they used GO to prevent the aggregation of MWCNTs. Furthermore, overpotential was reduced and the peak current of AA oxidation was increased by positively charged AuNRs. The electrochemical properties of biosensors were investigated by cyclic voltammetry (CV). Finally, this ascorbic acid biosensor sensitively detected ascorbic acid with low working potential (0.036 V), low detection limit (0.85 nM), and high sensitivity ($7.61 \mu\text{A } \mu\text{M}^{-1} \text{ cm}^{-2}$).

CNTs can be applied as biosensors for the detection of uric acid and it has already been proven in several studies [124][125][126]. Some chronically ill patients have hyperuricemia, in which there is too much uric acid in the body [127]. It accumulates in the cartilages and produces tophi and uric acid crystals, which cause great pain to the patient. In addition, the accumulation of tophi and uric acid induces an inflammatory response in the cartilages and causes lasting damage to cartilage and bones [128]. This phenomenon also entails great pain for the patient. Tophi and uric acid accumulate in the kidneys as well as in the cartilages, and just as they accumulate in the cartilages, they cause very severe organ irritation and pain [129]. For the detection of uric acid, Huang B et al. reported a standing electrochemical sensor based on CNT for

the determination of uric acid [130]. They developed a free-standing electrochemical biosensor. CNT was modified with 3D graphene foam (GF) and gold nanoparticles (GNPs) for the fabrication of biosensors (GF/CNTs/GNPs). Cyclic voltammetry (CV) and differential pulse voltammetry (DPV) were used for the investigation of the electrochemical properties of GF/CNTs/GNPs. GF/CNTs/GNPs show outstanding electrocatalytic activity toward dopamine and uric acid. Detection of uric acid with GF/CNTs/GNPs shows remarkable sensitivity of $3.36 \mu\text{A } \mu\text{M}^{-1} \text{ cm}^{-2}$, the low detection limits of 33.03 nM (S/N = 3), with a wide linear range of 0.50–60 μM . Furthermore, GF/CNTs/GNPs evaluated the quantification of uric acid with human urine. GF/CNTs/GNPs show good agreement in the concentration of uric acid (μM), total found (μM), and recovery (%) with high-performance liquid chromatography.

CNT-based biosensors can detect not only single molecules but also protein-based components. Here, researchers introduce the detection of biological components for the diagnosis of Alzheimer's disease. Amyloid- β accumulates in the brains of people with Alzheimer's disease and this phenomenon is a pathological mechanism of Alzheimer's disease [131]. Amyloid precursor protein is one of the proteins that plays a very important role in regulating the homeostasis of the neuronal system, such as neuronal development and signal transfer between neurons [132]. However, various precursor protein cleavage products produced by the cleavage of amyloid precursor protein are very closely related to Alzheimer's disease and induce dysfunction of the neuronal system [133]. Oh, J et al. reported a carbon nanotube (CNT) film-based biosensor with a metal-semiconductor field effect transistor structure (MESFET) for amyloid- β detection in human serum [134]. Briefly, for the fabrication of CNT-MESFET, the top gate was modified by depositing Au (10 nm) only in the middle of the semiconducting CNT channel. These immobilized antibodies on CNT-MESFETs were controlled by the antibody-binding proteins. In order to detect HRP used as the model analyte, anti-HRP antibodies were immobilized on the Au top gate with protein G or auto-displayed Zdomains of protein A as the antibody-binding protein. CNT-MESFET exhibited a higher sensitivity than the antibodies immobilized biosensor using a chemical linker. CNT-MESFET could detect the HRP at levels as low as 1 fg mL^{-1} in serum. Finally, they applied the CNT-MESFET to the detection of amyloid- β in human serum. This CNT-MESFET could detect the amyloid- β at the level of 1 pg mL^{-1} in human serum. It can be applied as a CNT-based biological material detection sensor with very high sensitivity, and further research is needed to see if it can detect other substances besides amyloid- β .

Thrombin is a protein closely related to blood clotting [135]. During bleeding, platelets are destroyed, and thromboplastin is released into the plasma, which is activated in the presence of calcium ions in the blood and becomes thrombin. It catalyzes the reaction of hydrolysis of soluble fibrinogen in the blood, which is the essence of blood coagulation, into insoluble fibrin [136]. Therefore, quantitative detection of thrombin in bleeding patients or patients undergoing surgery can prevent accidents caused by bleeding and judge the patient's condition for bleeding more clearly. Su, Z et al. reported an amperometric thrombin aptamer sensor (aptasensor) as a thrombin biosensor [91]. For the fabrication of the aptasensor, polyaniline-coated MWCNT was placed on the glassy carbon electrode (GCE). Later thiolated thrombin-specific aptamers were conjugated with polyaniline by the thiol-ene reaction. The surface of the aptasensor was coated with bovine serum albumin to prevent non-specific binding. The modified GCE shows a pair of well-defined redox peaks (at 50/–25 mV) and the tethered TTA–thrombin interaction shows a decreased electrochemical signal. Thrombin in spiked human serum (0.2 to 4 nM) was accurately detected by the aptasensor and it shows recoveries that ranged from 95 to 102%.

Accurately detecting COVID-19 is very important in the situation of the pandemic. Early detection and accurate diagnosis of the virus can prevent the spread of coronavirus infection. In addition, diagnosis of severe acute respiratory syndrome coronavirus 2 (SARS-CoV-2) is crucial for tracking the route of transmission and suitable treatment for patients in the event of a pandemic [137][138]. Pinals, R et al. introduced an SWCNT-based optical sensing approach toward this end [105]. SARS-CoV-2 enters the host cell through binding to the ACE2 receptor [139]. They used ACE2 to fabricate the noncovalently functionalized SWCNT as a virus sensor since ACE2 has a high binding affinity to the SARS-CoV-2 spike protein. Biosensor fluorescence was increased (2-fold) in the presence of the SARS-CoV-2 spike protein. They evaluated biosensor stability and confirmed preserving sensing responses in saliva and virus delivery media. In addition, it was demonstrated that the biosensor had a 73% fluorescence-on response within 5 s of exposure to 35 mg L^{-1} SARS-CoV-2 virus-like particles. The biosensor shows a 100% turn-on response in fluorescence upon the addition of $1 \mu\text{M}$ CoV-2 S spike protein receptor-binding domain (S RBD).

Zamzami, M et al. developed a fast (2–3 min), easy-to-use, low-cost, and quantitative electrochemical biosensor based on a CNT field-effect transistor (CNT-FET) that allows digital detection of the SARS-CoV-2 S1 [28]. It can quickly and accurately detect SARS-CoV-2 S1 antigens in saliva samples. The anti-SARS-CoV-2 S1 was immobilized on a Si/SiO₂ surface by CNT printing for the fabrication of a CNT-FET biosensor. The CNT-FET biosensor effectively detected the SARS-CoV-2 S1 antigen in 10 mM ammonium acetate buffer at concentrations from 0.1 fg mL^{-1} to 5.0 pg mL^{-1} . The limit of detection (LOD) of the CNT-FET biosensor was 4.12 fg mL^{-1} . In order to confirm whether the biosensor can specifically detect only the target antigen, selectivity tests were performed using target SARS-CoV-2 S1 and non-target SARS-CoV-1

S1 and MERS-CoV S1 antigens. The biosensor has good detection sensitivity with SARS-CoV-2 S1 antigen. However, it shows no detection response to SARS-CoV-1 S1 and MERS-CoV S1 antigen. The developed CNT-FET biosensor was verified to be capable of sensitive, fast, and accurate detection of SARS-CoV-2 S1 in human saliva.

3.4. Carbon Nanotube for Bacteria and Virus Detection

As mentioned before, CNTs and their derived structures have excellent physical properties including electrical conductivity, SERS, FRET, and so on. They can be utilized as sensing channels to detect bacteria, viruses, virus DNA, etc. [140][141]. Especially, the need for high-performance virus sensing platforms has increased for well-being and better human life, so many CNT-based sensing systems have been introduced. For example, Lee and his co-workers introduced virus DNA detection via an electrical biosensing platform which is composed of magnetically aligned NPs decorated CNT on the IDE [142]. In the study, firstly gold and magnetic nanoparticles were modified on the surface of CNT (Au/MNP-CNT) and they were laid on the Pt-IDE via an external magnetic field. After that, the thiol-modified probe DNA was immobilized on the Au NP. In this case, Au and CNT played a role as electrical sensing channels and MNP was the moiety for alignment. Due to the synergic properties between the three nanomaterials, this sensing platform showed high sensitivity with a LOD of 8.4 pM for influenza virus DNA and 8.8 pM for norovirus DNA. Furthermore, it showed high selectivity against mismatched DNA strains. Therefore, this sensing platform could show excellent sensing performance.

On the other hand, metallic nanoparticles (NPs)-decorated CNT was also used as a plasmonic substrate for a plasmonic resonance energy transfer (PRET)-based FL immune sensing system. In this case, metallic NPs such as gold or silver NPs and CNT possess plasmonic properties; thus, their hybrid structure-based plasmonic material has synergic properties. For instance, the plasmonic property of gold NP-decorated CNT (gold-CNT) assisted in the detection of influenza viruses [143]. In the study, gold-CNT was modified with influenza virus Ab, so it could capture the target virus and subsequently, fluorescent quantum dots (QDs)-Ab were added into the mixture and bound with virus-Ab-gold CNTs, and finally, sandwich structures were induced. As a result, depending on the concentrations of the target influenza virus, the FL of QD was changed linearly. According to the results of detection performance, the limit of detection of viruses was estimated at around 0.1 pg mL⁻¹. Furthermore, the influenza virus from a clinical sample was also monitored with excellent sensitivity was 50 PFU mL⁻¹ in the range of 50–10,000 PFU mL⁻¹. It meant that a metal NP-CNT structure-based fluoro-immuno sensing system could be potentially applied for virus detection.

In another study, CNT could be utilized as a sensing channel to detect the dengue virus (DENV) via an electrochemical approach. Wasik et al. fabricated a heparin-SWCNT hybrid structure on the electrode to monitor the dengue virus and the resistance difference was measured depending on the concentration of the virus [144]. The limit of detection of this system showed 8 DENV/chip and this system showed excellent selectivity against the influenza virus. Therefore, a CNT-based electrochemical sensing platform also could be developed for high-performance biosensors.

On the other hand, some bacteria have caused critical diseases, and they have threatened human life. So, a highly sensitive and selective bacteria sensing system was required, and several bacteria were also successfully detected by using a CNT-based sensing platform. For instance, Zhang et al. reported a gold-CNT-based sensing system that could detect *Escherichia coli* (*E. coli*) through an electrochemical approach [145]. Firstly, they fabricated the gold-CNT/GCE for the sensing channel. Then, the captured Ab was immobilized on the surface of gold-CNT to monitor the *E. coli*. The sensing behavior of the gold-CNT-based sensing system was characterized depending on the amounts of bacteria from 2.0×10^2 to 2.0×10^6 CFU mL⁻¹. This system showed linear response depending on the amount of *E. coli* and good sensitivity and selectivity was also proven. Especially, *E. coli* in sludge was also successfully detected, thus this system exhibited excellent sensing performance.

In another study, the detection of *E. coli* O157:H7 based on an MWCNT electrical sensing system was introduced by Li and co-workers [146]. In the study, MWCNT was covered by polystyrene sulfonate (PSS) and the authors produced a PSS-MWCNT-based layer-by-layer (LBL) structure using poly(ethyleneimine) (PEI) to apply for the electrical sensing channel. O157:H7 Abs were modified on the surface of MWCNT to capture the target bacteria. The electrical signal was monitored depending on the concentration of O157:H7 and a linear response was shown. Interestingly, the authors collected the bacteria that were captured (O157:H7) by the sensing channel and isolated specific DNA from the collected O157:H7. Subsequently, the concentration of O157:H7 DNA was estimated by loop-mediated isothermal amplification (LAMP). Based on the sensing performance results, the LOD of this system was around 1 PFU mL⁻¹. Therefore, they developed highly sensitive bacteria detection systems using MWCNT.

E. coli in dairy products were also detected by using CNT and gold NP mixture [147]. In this case, the surface of CNT was modified with target Ab by an EDC/NHS coupling reaction and horseradish peroxidase (HRP) enzyme at the same time. On the other hand, gold NPs were coated by poly(amidoamine) dendrimer and specific Ab for *E. coli* was attached to the

surface of NPs. In this environment, if target bacteria existed in the sample, these two nanomaterials could be formed as a sandwich structure with bacteria and its electrochemical sensing signal might be changed. The sensing performance of this system was tested under a range of 1.0×10^2 to 1.0×10^6 CFU mL⁻¹ and a LOD of around 50 CFU mL⁻¹ was estimated. Therefore, a CNT-based sensing system could be applied to the bacteria screening platform.

Liu et al. have reported that molecular imprinted TiO₂-coated multiwalled carbon nanotubes (MI-TiO₂@CNTs) were fabricated to detect microcystin-LR (MC-LR), a type of cyanobacterial toxin in water by the photoelectrochemical method. The molecular imprinted TiO₂ showed enhanced detection in comparison to traditional TiO₂ and non-imprinted TiO₂. This sensor resulted in a wide linear range from 1.0 pM to 3.0 nM for the detection of MC-LR. MI-TiO₂@CNTs achieved magnificent selectivity towards MC-LR. Moreover, this promising sensor showed high sensitivity for the detection of MC-LR which could be a potential candidate for water purification [29].

He and co-workers developed an enzyme-free and dual-signal readout immunosensor that was used to detect MC-LR while an enzyme-based biosensor with great obstacles such as instability, sensitivity, temperature, and pH should be considered. Initially, gold nanoparticle-decorated CNT (AgNP-CNTs) was fabricated for the detection of MC-LR and secondly, silver nanorods were coated over AgNP-CNTs to detect via dual-signal mode. These sensors showed the determination of MC-LR in a linear range from 0.005 µg L⁻¹ to 20 µg L⁻¹ with a LOD of 2.8 ng L⁻¹. In terms of reproducibility, high selectivity, and sensitivity, these sensors indicated their promising application in environment monitoring [148].

In another study, Han et al. proposed an MWCNT-based electrochemical biosensor that was demonstrated to monitor the MC-LR in drinking water supplies. This biosensor was fabricated in well-aligned and millimeter-long MWCNT arrays by water-assisted CVD. In addition, monoclonal antibodies were decorated to specify MC-LR toxin detection. A linear range from 0.05 to 20 µg L⁻¹ was observed for the detection of MC-LR with a LOD of 1 µg L⁻¹ in drinking water [149]. To reduce the burden of cost-effectiveness and increase the rapid detection of MC-LR in environmental water, Queiros and co-workers proposed label-free potentiometric sensors composed of MWCNTs. These sensors were synthesized by imprinted polymer and polyvinyl chloride membranes. This method was applied successfully to detect MC-LR with great selectivity and sensitivity. Moreover, this method benefited with easy production and cost-effectiveness [150].

Cholera is another devastating disease that has taken uncountable lives over the past few decades. The detection of cholera toxin (CT) was highly required to eradicate cholera from our lives. Viswanathan et al. proposed a sensitive method to detect CT by using an electrochemical immunosensor. This immunosensor was composed of potassium ferrocyanide, ganglioside (GM1)-functionalized liposomes, and monoclonal antibodies on the surface of Nafion-supported multi-walled carbon nanotubes. The detection mechanism was proposed by a sandwich-type assay, where the toxin was first coupled with an anti-CT antibody and followed by a GM1-functionalized liposome. This sandwich method resulted in the detection of CT in ultra-trace levels. The detection of CT showed a linear range of 10^{-14} – 10^{-7} g mL⁻¹ with a LOD of 10^{-16} g of CT [151].

In another study, Palomar et al. proposed an impedimetric immunosensor based on CNTs to improve sensing performances by increasing electroactive surface areas on CNTs. These systems were modified with polypyrrole-nitrilotriacetic acid (poly(pyrrole-NTA)) and Cu (II) complex to produce sensor devices. With great sensitivity and easy reproducibility, the cholera sensor showed a promising linear detection range from 10^{-13} – 10^{-5} g mL⁻¹ with a LOD of 10^{-13} g mL⁻¹, which could be a potential sensing platform to detect cholera in the environment [152].

4. Conclusions

Over the years, researchers and scientists have used a diverse range of nanomaterials such as metal nanoparticles (NPs), metal oxide NPs, nanofibers [153], quantum dots (QDs), and carbon nanomaterials such as carbon quantum dots [154], graphene, and carbon nanotubes (CNTs) to fabricate high-performance and sensitive biosensors. CNTs and their derivatives have gained great attention in the field of advanced functional materials today. It has been explored in diverse fields from defense to electronics. The field of biomedical applications has investigated CNTs and their derivatives extensively as potential candidates. Although the physical and chemical properties are not completely understood, it has been exploited by the electronics industry over the years. CNTs showed excellent properties in device fabrications as well as sensing behaviors. CNTs and their derivatives have been utilized for bio and chemical sensing due to having similar sizes to the analytes and bio-species. Due to their small size and high aspect ratio, CNTs exhibit unusual optical, mechanical, electrical, and chemical properties due to their small diameter and high aspect ratio. Utilizing them, a wide class of sensors is fabricated. It has been shown that CNTs have improved cell penetration properties and stability, as well as chirality and diameter-based physicochemical properties. On the account of synthesis, the materials that are necessary

for CNT production are profuse, and they can be crafted with only a modest amount of raw materials. Further functionalization without damaging the covalent backbone extends the desired application of CNTs. Although one major drawback of CNT production is reproducibility, structurally and chemically reproducible batch production with minimal impurities is an immediate concern. Another two important properties that distinguish them from other nanomaterials are temperature stability (2800 °C in vacuum and ~750 °C in air) and hydrophilicity. While considering the mechanical properties, extremely high Young's modulus values (1–1.8 TPa range) allow them to act as an excellent candidate for probe tips for scanning microscopy. Although some other disadvantages are always associated with CNTs, namely cellular toxicity, incompatibility with biological mediums, agglomeration, accumulation, and long-term persistence which require a strong action for mitigation. Numerous studies on CNTs and their derivatives have reported their interactions with analytes and their toxicology profiles. However, to allow their commercialization, there are limits in terms of cost-effectiveness, purity, and high density of perfect alignment during industrialization. A huge number of studies are conducted on biosensors to enable their commercialization. Interestingly, CNTs have been investigated as biosensors as in vivo devices, while many efforts have been made to minimize their toxicity profile.

References

1. Justino, C.I.L.; Rocha-Santos, T.A.; Duarte, A.C.; Rocha-Santos, T.A. Review of Analytical Figures of Merit of Sensors and Biosensors in Clinical Applications. *TrAC Trends Anal. Chem.* 2010, 29, 1172–1183.
2. Guo, S.; Dong, S. Biomolecule-Nanoparticle Hybrids for Electrochemical Biosensors. *TrAC Trends Anal. Chem.* 2009, 28, 96–109.
3. Chen, X.; Van Pée, K.-H. Catalytic Mechanisms, Basic Roles, and Biotechnological and Environmental Significance of Halogenating Enzymes. *Acta Biochim. Biophys. Sin.* 2008, 40, 183–193.
4. Cornell, B.A.; Braach-Maksvytis, V.L.B.; King, L.G.; Osman, P.D.J.; Raguse, B.; Wieczorek, L.; Pace, R.J. A Biosensor That Uses Ion-Channel Switches. *Nature* 1997, 387, 580–583.
5. Luong, J.H.T.; Male, K.B.; Glennon, J.D. Biosensor Technology: Technology Push versus Market Pull. *Biotechnol. Adv.* 2008, 26, 492–500.
6. Bhalla, N.; Jolly, P.; Formisano, N.; Estrela, P. Introduction to Biosensors. *Essays Biochem.* 2016, 60, 1–8.
7. Thévenot, D.R.; Toth, K.; Durst, R.A.; Wilson, G.S. Electrochemical Biosensors: Recommended Definitions and Classification. *Anal. Lett.* 2001, 34, 635–659.
8. Dincer, C.; Bruch, R.; Costa-Rama, E.; Fernández-Abedul, M.T.; Merkoçi, A.; Manz, A.; Urban, G.A.; Güder, F. Disposable Sensors in Diagnostics, Food, and Environmental Monitoring. *Adv. Mater.* 2019, 31, 1806739.
9. Lee, J.; Lee, J.-H.; Mondal, J.; Hwang, J.; Kim, H.S.; Kumar, V.; Raj, A.; Hwang, S.R.; Lee, Y.-K. Magnetofluoro-Immunosensing Platform Based on Binary Nanoparticle-Decorated Graphene for Detection of Cancer Cell-Derived Exosomes. *Int. J. Mol. Sci.* 2022, 23, 9619.
10. Sireesha, M.; Jagadeesh Babu, V.; Kranthi Kiran, A.S.; Ramakrishna, S. A Review on Carbon Nanotubes in Biosensor Devices and Their Applications in Medicine. *Nanocomposites* 2018, 4, 36–57.
11. Kundu, M.; Krishnan, P.; Kotnala, R.K.; Sumana, G. Recent Developments in Biosensors to Combat Agricultural Challenges and Their Future Prospects. *Trends Food Sci. Technol.* 2019, 88, 157–178.
12. Eivazzadeh-Keihan, R.; Pashazadeh, P.; Hejazi, M.; de la Guardia, M.; Mokhtarzadeh, A. Recent Advances in Nanomaterial-Mediated Bio and Immune Sensors for Detection of Aflatoxin in Food Products. *TrAC Trends Anal. Chem.* 2017, 87, 112–128.
13. Theuer, L.; Randek, J.; Junne, S.; Neubauer, P.; Mandenius, C.-F.; Beni, V. Single-Use Printed Biosensor for L-Lactate and Its Application in Bioprocess Monitoring. *Processes* 2020, 8, 321.
14. Cennamo, N.; Zeni, L.; Tortora, P.; Regonesi, M.E.; Giusti, A.; Staiano, M.; D'Auria, S.; Varriale, A. A High Sensitivity Biosensor to Detect the Presence of Perfluorinated Compounds in Environment. *Talanta* 2018, 178, 955–961.
15. Meshram, B.D.; Agrawal, A.K.; Adil, S.; Ranvir, S.; Sande, K.K. Biosensor and Its Application in Food and Dairy Industry: A Review. *Int. J. Curr. Microbiol. Appl. Sci.* 2018, 7, 3305–3324.
16. Peng, B.; Locascio, M.; Zapol, P.; Li, S.; Mielke, S.L.; Schatz, G.C.; Espinosa, H.D. Measurements of Near-Ultimate Strength for Multiwalled Carbon Nanotubes and Irradiation-Induced Crosslinking Improvements. *Nat. Nanotechnol.* 2008, 3, 626–631.
17. Wang, J. Carbon-Nanotube Based Electrochemical Biosensors: A Review. *Electroanalysis* 2005, 17, 7–14.

18. Yun, Y.; Dong, Z.; Shanov, V.; Heineman, W.R.; Halsall, H.B.; Bhattacharya, A.; Conforti, L.; Narayan, R.K.; Ball, W.S.; Schulz, M.J. Nanotube Electrodes and Biosensors. *Nano Today* 2007, 2, 30–37.
19. Thirumalraj, B.; Kubendhiran, S.; Chen, S.-M.; Lin, K.-Y. Highly Sensitive Electrochemical Detection of Palmatine Using a Biocompatible Multiwalled Carbon Nanotube/Poly-L-Lysine Composite. *J. Colloid Interface Sci.* 2017, 498, 144–152.
20. Singh, S.; Vardharajula, S.; Tiwari, P.; Eroğlu, E.; Vig, K.; Dennis, V. Ali Functionalized Carbon Nanotubes: Biomedical Applications. *Int. J. Nanomed.* 2012, 7, 5361.
21. Bianco, A.; Kostarelos, K.; Partidos, C.D.; Prato, M. Biomedical Applications of Functionalised Carbon Nanotubes. *Chem. Commun.* 2005, 5, 571.
22. Kam, N.W.S.; Liu, Z.; Dai, H. Functionalization of Carbon Nanotubes via Cleavable Disulfide Bonds for Efficient Intracellular Delivery of SiRNA and Potent Gene Silencing. *J. Am. Chem. Soc.* 2005, 127, 12492–12493.
23. Tîlmaciu, C.-M.; Morris, M.C. Carbon Nanotube Biosensors. *Front. Chem.* 2015, 3, 59.
24. Malhotra, B.D.; Ali, M.A. Nanomaterials in Biosensors. In *Nanomaterials for Biosensors*; Elsevier: Amsterdam, The Netherlands, 2018; pp. 1–74.
25. Balasubramanian, K.; Burghard, M. Biosensors Based on Carbon Nanotubes. *Anal. Bioanal. Chem.* 2006, 385, 452–468.
26. Jacobs, C.B.; Peairs, M.J.; Venton, B.J. Review: Carbon Nanotube Based Electrochemical Sensors for Biomolecules. *Anal. Chim. Acta* 2010, 662, 105–127.
27. Jin, Q.; Dai, M.; Zhan, X.; Wang, S.; He, Z. Carbon Nanotubes and Graphene Composites Used in Cr(VI) Detection Techniques: A Review. *J. Alloys Compd.* 2022, 922, 166268.
28. Zamzami, M.A.; Rabbani, G.; Ahmad, A.; Basalah, A.A.; Al-Sabban, W.H.; Nate Ahn, S.; Choudhry, H. Carbon Nanotube Field-Effect Transistor (CNT-FET)-Based Biosensor for Rapid Detection of SARS-CoV-2 (COVID-19) Surface Spike Protein S1. *Bioelectrochemistry* 2022, 143, 107982.
29. Liu, M.; Ding, X.; Yang, Q.; Wang, Y.; Zhao, G.; Yang, N. A PM Leveled Photoelectrochemical Sensor for Microcystin-LR Based on Surface Molecularly Imprinted TiO₂@CNTs Nanostructure. *J. Hazard. Mater.* 2017, 331, 309–320.
30. Aasi, A.; Aasi, E.; Mehdi Aghaei, S.; Panchapakesan, B. CNT Biodevices for Early Liver Cancer Diagnosis Based on Biomarkers Detection- a Promising Platform. *J. Mol. Graph. Model.* 2022, 114, 108208.
31. Ahmadian, E.; Janas, D.; Eftekhari, A.; Zare, N. Application of Carbon Nanotubes in Sensing/Monitoring of Pancreas and Liver Cancer. *Chemosphere* 2022, 302, 134826.
32. Lin, M.-H.; Gupta, S.; Chang, C.; Lee, C.-Y.; Tai, N.-H. Carbon Nanotubes/Polyethylenimine/Glucose Oxidase as a Non-Invasive Electrochemical Biosensor Performs High Sensitivity for Detecting Glucose in Saliva. *Microchem. J.* 2022, 180, 107547.
33. Anand, U.; Chandel, A.K.S.; Oleksak, P.; Mishra, A.; Krejcar, O.; Raval, I.H.; Dey, A.; Kuca, K. Recent Advances in the Potential Applications of Luminescence-Based, SPR-Based, and Carbon-Based Biosensors. *Appl. Microbiol. Biotechnol.* 2022, 106, 2827–2853.
34. Kroto, H.W.; Heath, J.R.; O'Brien, S.C.; Curl, R.F.; Smalley, R.E. C₆₀: Buckminsterfullerene. *Nature* 1985, 318, 162–163.
35. Iijima, S. Helical Microtubules of Graphitic Carbon. *Nature* 1991, 354, 56–58.
36. Iijima, S.; Ichihashi, T. Single-Shell Carbon Nanotubes of 1-Nm Diameter. *Nature* 1993, 363, 603–605.
37. Bethune, D.S.; Kiang, C.H.; de Vries, M.S.; Gorman, G.; Savoy, R.; Vazquez, J.; Beyers, R. Cobalt-Catalysed Growth of Carbon Nanotubes with Single-Atomic-Layer Walls. *Nature* 1993, 363, 605–607.
38. Arora, N.; Sharma, N.N. Arc Discharge Synthesis of Carbon Nanotubes: Comprehensive Review. *Diam. Relat. Mater.* 2014, 50, 135–150.
39. Gamaly, E.G.; Ebbesen, T.W. Mechanism of Carbon Nanotube Formation in the Arc Discharge. *Phys. Rev. B* 1995, 52, 2083–2089.
40. De Heer, W.A.; Poncharal, P.; Berger, C.; Gezo, J.; Song, Z.; Bettini, J.; Ugarte, D. Liquid Carbon, Carbon-Glass Beads, and the Crystallization of Carbon Nanotubes. *Science* 2005, 307, 907–910.
41. Ugarte, D. High-Temperature Behaviour of “Fullerene Black”. *Carbon N. Y.* 1994, 32, 1245–1248.
42. Zhou, D.; Chow, L. Complex Structure of Carbon Nanotubes and Their Implications for Formation Mechanism. *J. Appl. Phys.* 2003, 93, 9972–9976.

43. Doherty, S.P.; Chang, R.P.H. Synthesis of Multiwalled Carbon Nanotubes from Carbon Black. *Appl. Phys. Lett.* 2002, 81, 2466–2468.
44. Doherty, S.P.; Buchholz, D.B.; Li, B.-J.; Chang, R.P.H. Solid-State Synthesis of Multiwalled Carbon Nanotubes. *J. Mater. Res.* 2003, 18, 941–949.
45. Doherty, S.P.; Buchholz, D.B.; Chang, R.P.H. Semi-Continuous Production of Multiwalled Carbon Nanotubes Using Magnetic Field Assisted Arc Furnace. *Carbon N. Y.* 2006, 44, 1511–1517.
46. Chen, Z.-G.; Li, F.; Ren, W.-C.; Cong, H.; Liu, C.; Lu, G.Q.; Cheng, H.-M. Double-Walled Carbon Nanotubes Synthesized Using Carbon Black as the Dot Carbon Source. *Nanotechnology* 2006, 17, 3100–3104.
47. Sano, N.; Nakano, J.; Kanki, T. Synthesis of Single-Walled Carbon Nanotubes with Nanohorns by Arc in Liquid Nitrogen. *Carbon N. Y.* 2004, 42, 686–688.
48. Shang, H.; Xie, H.; Zhu, H.; Dai, F.; Wu, D.; Wang, W.; Fang, Y. Investigation of Strain in Individual Multi-Walled Carbon Nanotube by a Novel Moiré Method. *J. Mater. Process. Technol.* 2005, 170, 108–111.
49. Tripathi, G.; Tripathi, B.; Sharma, M.K.; Vijay, Y.K.; Chandra, A.; Jain, I.P. A Comparative Study of Arc Discharge and Chemical Vapor Deposition Synthesized Carbon Nanotubes. *Int. J. Hydrogen Energy* 2012, 37, 3833–3838.
50. Zhao, J.; Wei, L.; Yang, Z.; Zhang, Y. Continuous and Low-Cost Synthesis of High-Quality Multi-Walled Carbon Nanotubes by Arc Discharge in Air. *Phys. E Low-Dimens. Syst. Nanostruct.* 2012, 44, 1639–1643.
51. Keidar, M.; Levchenko, I.; Arbel, T.; Alexander, M.; Waas, A.M.; Ostrikov, K. (Ken) Increasing the Length of Single-Wall Carbon Nanotubes in a Magnetically Enhanced Arc Discharge. *Appl. Phys. Lett.* 2008, 92, 043129.
52. Keidar, M.; Levchenko, I.; Arbel, T.; Alexander, M.; Waas, A.M.; Ostrikov, K.K. Magnetic-Field-Enhanced Synthesis of Single-Wall Carbon Nanotubes in Arc Discharge. *J. Appl. Phys.* 2008, 103, 094318.
53. Tang, D.; Xie, S.; Zhou, W.; Liu, Z.; Ci, L.; Yan, X.; Yuan, H.; Zhou, Z.; Liang, Y.; Liu, D.; et al. Effect of Cupped Cathode on Microstructures of Carbon Nanotubes in Arc Discharge. *Carbon N. Y.* 2002, 40, 1609–1613.
54. Shimotani, K.; Anazawa, K.; Watanabe, H.; Shimizu, M. New Synthesis of Multi-Walled Carbon Nanotubes Using an Arc Discharge Technique under Organic Molecular Atmospheres. *Appl. Phys. A* 2001, 73, 451–454.
55. Yousef, S.; Khattab, A.; Osman, T.A.; Zaki, M. Effects of Increasing Electrodes on CNTs Yield Synthesized by Using Arc-Discharge Technique. *J. Nanomater.* 2013, 2013, 1–9.
56. Roch, A.; Jost, O.; Schultrich, B.; Beyer, E. High-Yield Synthesis of Single-Walled Carbon Nanotubes with a Pulsed Arc-Discharge Technique. *Phys. Status Solidi* 2007, 244, 3907–3910.
57. Okada, T.; Kaneko, T.; Hatakeyama, R. Conversion of Toluene into Carbon Nanotubes Using Arc Discharge Plasmas in Solution. *Thin Solid Film.* 2007, 515, 4262–4265.
58. Wang, Y.-H.; Chiu, S.-C.; Lin, K.-M.; Li, Y.-Y. Formation of Carbon Nanotubes from Polyvinyl Alcohol Using Arc-Discharge Method. *Carbon N. Y.* 2004, 42, 2535–2541.
59. Horváth, Z.E.; Kertész, K.; Pethő, L.; Koós, A.A.; Tapasztó, L.; Vértesy, Z.; Osváth, Z.; Darabont, A.; Nemes-Incze, P.; Sárközi, Z.; et al. Inexpensive, Upscalable Nanotube Growth Methods. *Curr. Appl. Phys.* 2006, 6, 135–140.
60. Ren, F.; Kanaan, S.A.; Majewska, M.M.; Keskar, G.D.; Azoz, S.; Wang, H.; Wang, X.; Haller, G.L.; Chen, Y.; Pfefferle, L.D. Increase in the Yield of (and Selective Synthesis of Large-Diameter) Single-Walled Carbon Nanotubes through Water-Assisted Ethanol Pyrolysis. *J. Catal.* 2014, 309, 419–427.
61. Ando, Y.; Zhao, X.; Sugai, T.; Kumar, M. Growing Carbon Nanotubes. *Mater. Today* 2004, 7, 22–29.
62. ChandraKishore, S.; Pandurangan, A. Electrophoretic Deposition of Cobalt Catalyst Layer over Stainless Steel for the High Yield Synthesis of Carbon Nanotubes. *Appl. Surf. Sci.* 2012, 258, 7936–7942.
63. Ahmad, S.; Liao, Y.; Hussain, A.; Zhang, Q.; Ding, E.-X.; Jiang, H.; Kauppinen, E.I. Systematic Investigation of the Catalyst Composition Effects on Single-Walled Carbon Nanotubes Synthesis in Floating-Catalyst CVD. *Carbon N. Y.* 2019, 149, 318–327.
64. Hoecker, C.; Smail, F.; Pick, M.; Boies, A. The Influence of Carbon Source and Catalyst Nanoparticles on CVD Synthesis of CNT Aerogel. *Chem. Eng. J.* 2017, 314, 388–395.
65. Barnard, J.S.; Paukner, C.; Koziol, K.K. The Role of Carbon Precursor on Carbon Nanotube Chirality in Floating Catalyst Chemical Vapour Deposition. *Nanoscale* 2016, 8, 17262–17270.
66. Abdullah, H.B.; Irmawati, R.; Ismail, I.; Yusof, N.A. Utilization of Waste Engine Oil for Carbon Nanotube Aerogel Production Using Floating Catalyst Chemical Vapor Deposition. *J. Clean. Prod.* 2020, 261, 121188.
67. Guo, J.; Jiang, H.; Teng, Y.; Xiong, Y.; Chen, Z.; You, L.; Xiao, D. Recent Advances in Magnetic Carbon Nanotubes: Synthesis, Challenges and Highlighted Applications. *J. Mater. Chem. B* 2021, 9, 9076–9099.

68. Rangreez, T.A.; Mobin, R.; Chisti, H.T.N. Potentiometric Determination of Mercury Ions by Sol-Gel Synthesized Multi-Walled Carbon Nanotubes Zr (IV) Phosphate Composite Fabricated Membrane Electrode. *Curr. Anal. Chem.* 2022, 18, 466–474.
69. Safaei, B.; How, H.C.; Scribano, G. A Computational Study on Synthesis of Carbon Nanotubes in a Sooty Inverse Diffusion Flame. *Int. J. Environ. Sci. Technol.* 2022.
70. Lee, T.; Teng, T.Z.J.; Shelat, V.G. Carbohydrate Antigen 19-9—Tumor Marker: Past, Present, and Future. *World J. Gastrointest. Surg.* 2020, 12, 468–490.
71. Będkowska, G.E.; Gacuta, E.; Zbucka-Krętowska, M.; Ławicki, P.; Szmitkowski, M.; Lemancewicz, A.; Motyka, J.; Kobus, A.; Choraży, M.; Paniczko, M.; et al. Plasma Levels and Diagnostic Utility of VEGF in a Three-Year Follow-Up of Patients with Breast Cancer. *J. Clin. Med.* 2021, 10, 5452.
72. Cash, K.J.; Clark, H.A. Nanosensors and Nanomaterials for Monitoring Glucose in Diabetes. *Trends Mol. Med.* 2010, 16, 584–593.
73. Taguchi, M.; Ptitsyn, A.; McLamore, E.S.; Claussen, J.C. Nanomaterial-Mediated Biosensors for Monitoring Glucose. *J. Diabetes Sci. Technol.* 2014, 8, 403–411.
74. Hassan, M.H.; Vyas, C.; Grieve, B.; Bartolo, P. Recent Advances in Enzymatic and Non-Enzymatic Electrochemical Glucose Sensing. *Sensors* 2021, 21, 4672.
75. Adeniyi, O.; Nwahara, N.; Mwanza, D.; Nyokong, T.; Mashazi, P. Nanohybrid Electrocatalyst Based on Cobalt Phthalocyanine-Carbon Nanotube-Reduced Graphene Oxide for Ultrasensitive Detection of Glucose in Human Saliva. *Sens. Actuators B Chem.* 2021, 348, 130723.
76. Figueredo, F.; Garcia, P.T.; Cortón, E.; Coltro, W.K.T. Enhanced Analytical Performance of Paper Microfluidic Devices by Using Fe₃O₄ Nanoparticles, MWCNT, and Graphene Oxide. *ACS Appl. Mater. Interfaces* 2016, 8, 11–15.
77. Sun, Z.; Liu, H.; Wang, X. Thermal Self-Regulatory Intelligent Biosensor Based on Carbon-Nanotubes-Decorated Phase-Change Microcapsules for Enhancement of Glucose Detection. *Biosens. Bioelectron.* 2022, 195, 113586.
78. Rasmussen, J.; Langerman, H. Alzheimer's Disease—Why We Need Early Diagnosis. *Degener. Neurol. Neuromuscul. Dis.* 2019, 9, 123–130.
79. Newman-Toker, D.E.; Wang, Z.; Zhu, Y.; Nassery, N.; Saber Tehrani, A.S.; Schaffer, A.C.; Yu-Moe, C.W.; Clemens, G.D.; Fanai, M.; Siegal, D. Rate of Diagnostic Errors and Serious Misdiagnosis-Related Harms for Major Vascular Events, Infections, and Cancers: Toward a National Incidence Estimate Using the “Big Three”. *Diagnosis* 2021, 8, 67–84.
80. Zhang, X.; Cui, H.; Gui, Y.; Tang, J. Mechanism and Application of Carbon Nanotube Sensors in SF₆ Decomposed Production Detection: A Review. *Nanoscale Res. Lett.* 2017, 12, 177.
81. Li, C.; Shi, G. Carbon Nanotube-Based Fluorescence Sensors. *J. Photochem. Photobiol. C Photochem. Rev.* 2014, 19, 20–34.
82. Norizan, M.N.; Moklis, M.H.; Ngah Demon, S.Z.; Halim, N.A.; Samsuri, A.; Mohamad, I.S.; Knight, V.F.; Abdullah, N. Carbon Nanotubes: Functionalisation and Their Application in Chemical Sensors. *RSC Adv.* 2020, 10, 43704–43732.
83. Kohn, J. A rapid method of estimating blood-glucose ranges. *Lancet* 1957, 270, 119–121.
84. Free, A.H.; Free, H.M. Self Testing, an Emerging Component of Clinical Chemistry. *Clin. Chem.* 1984, 30, 829–838.
85. Wang, C.; Li, J.; Tan, R.; Wang, Q.; Zhang, Z. Colorimetric Method for Glucose Detection with Enhanced Signal Intensity Using ZnFe₂O₄–Carbon Nanotube–Glucose Oxidase Composite Material. *Analyst* 2019, 144, 1831–1839.
86. Kumari, A.; Rajeev, R.; Benny, L.; Sudhakar, Y.N.; Varghese, A.; Hegde, G. Recent Advances in Carbon Nanotubes-Based Biocatalysts and Their Applications. *Adv. Colloid Interface Sci.* 2021, 297, 102542.
87. Wang, C.; Wang, Q.; Tan, R. Preparation of Enzyme-Functionalized Carbon Nanotubes and Their Application in Glucose and Fe²⁺ Detection through “Turn on” and “Turn off” Approaches. *Analyst* 2018, 143, 4118–4127.
88. Wilson, T.A.; Musameh, M.; Kyrtzsis, I.L.; Zhang, J.; Bond, A.M.; Hearn, M.T.W. Enhanced NADH Oxidation Using Polytyramine/Carbon Nanotube Modified Electrodes for Ethanol Biosensing. *Electroanalysis* 2017, 29, 1985–1993.
89. Nishikimi, M.; Yagi, K. Molecular Basis for the Deficiency in Humans of Gulonolactone Oxidase, a Key Enzyme for Ascorbic Acid Biosynthesis. *Am. J. Clin. Nutr.* 1991, 54, 1203S–1208S.
90. Hahn, T.; Adams, W.; Williams, K. Is Vitamin C Enough? A Case Report of Scurvy in a Five-Year-Old Girl and Review of the Literature. *BMC Pediatr.* 2019, 19, 74.
91. Yimcharoen, M.; Kittikunnathum, S.; Suknikorn, C.; Nak-on, W.; Yeethong, P.; Anthony, T.G.; Bunpo, P. Effects of Ascorbic Acid Supplementation on Oxidative Stress Markers in Healthy Women Following a Single Bout of Exercise. *J.*

92. Carr, A.; Maggini, S. Vitamin C and Immune Function. *Nutrients* 2017, 9, 1211.
93. Spoelstra-de Man, A.M.E.; Elbers, P.W.G.; Oudemans-Van Straaten, H.M. Vitamin C. *Curr. Opin. Crit. Care* 2018, 24, 248–255.
94. Al-Niaimi, F.; Chiang, N.Y.Z. Topical Vitamin C and the Skin: Mechanisms of Action and Clinical Applications. *J. Clin. Aesthet. Dermatol.* 2017, 10, 14–17.
95. Travica, N.; Ried, K.; Sali, A.; Scholey, A.; Hudson, I.; Pipingas, A. Vitamin C Status and Cognitive Function: A Systematic Review. *Nutrients* 2017, 9, 960.
96. Zhao, Y.; Qin, J.; Xu, H.; Gao, S.; Jiang, T.; Zhang, S.; Jin, J. Gold Nanorods Decorated with Graphene Oxide and Multi-Walled Carbon Nanotubes for Trace Level Voltammetric Determination of Ascorbic Acid. *Microchim. Acta* 2019, 186, 17.
97. Chen, P.-Y.; Nien, P.-C.; Hu, C.-W.; Ho, K.-C. Detection of Uric Acid Based on Multi-Walled Carbon Nanotubes Polymerized with a Layer of Molecularly Imprinted PMAA. *Sens. Actuators B Chem.* 2010, 146, 466–471.
98. Hatefi-Mehrjardi, A.; Karimi, M.A.; Soleymanzadeh, M.; Barani, A. Highly Sensitive Detection of Dopamine, Ascorbic and Uric Acid with a Nanostructure of Dianix Yellow/Multi-Walled Carbon Nanotubes Modified Electrode. *Measurement* 2020, 163, 107893.
99. Jarošová, R.; McClure, S.E.; Gajda, M.; Jović, M.; Girault, H.H.; Lesch, A.; Maiden, M.; Waters, C.; Swain, G.M. Inkjet-Printed Carbon Nanotube Electrodes for Measuring Pyocyanin and Uric Acid in a Wound Fluid Simulant and Culture Media. *Anal. Chem.* 2019, 91, 8835–8844.
100. Gliozzi, M.; Malara, N.; Muscoli, S.; Mollace, V. The Treatment of Hyperuricemia. *Int. J. Cardiol.* 2016, 213, 23–27.
101. Ruggiero, C.; Cherubini, A.; Ble, A.; Bos, A.J.G.; Maggio, M.; Dixit, V.D.; Lauretani, F.; Bandinelli, S.; Senin, U.; Ferrucci, L. Uric Acid and Inflammatory Markers. *Eur. Heart J.* 2006, 27, 1174–1181.
102. Prasad Sah, O.S.; Qing, Y.X. Associations between Hyperuricemia and Chronic Kidney Disease: A Review. *Nephrourol. Mon.* 2015, 7, e27233.
103. Huang, B.; Liu, J.; Lai, L.; Yu, F.; Ying, X.; Ye, B.-C.; Li, Y. A Free-Standing Electrochemical Sensor Based on Graphene Foam-Carbon Nanotube Composite Coupled with Gold Nanoparticles and Its Sensing Application for Electrochemical Determination of Dopamine and Uric Acid. *J. Electroanal. Chem.* 2017, 801, 129–134.
104. Jack, C.R.; Knopman, D.S.; Jagust, W.J.; Petersen, R.C.; Weiner, M.W.; Aisen, P.S.; Shaw, L.M.; Vemuri, P.; Wiste, H.J.; Weigand, S.D.; et al. Tracking Pathophysiological Processes in Alzheimer's Disease: An Updated Hypothetical Model of Dynamic Biomarkers. *Lancet Neurol.* 2013, 12, 207–216.
105. Chen, G.; Xu, T.; Yan, Y.; Zhou, Y.; Jiang, Y.; Melcher, K.; Xu, H.E. Amyloid Beta: Structure, Biology and Structure-Based Therapeutic Development. *Acta Pharmacol. Sin.* 2017, 38, 1205–1235.
106. O'Brien, R.J.; Wong, P.C. Amyloid Precursor Protein Processing and Alzheimer's Disease. *Annu. Rev. Neurosci.* 2011, 34, 185–204.
107. Oh, J.; Yoo, G.; Chang, Y.W.; Kim, H.J.; Jose, J.; Kim, E.; Pyun, J.-C.; Yoo, K.-H. A Carbon Nanotube Metal Semiconductor Field Effect Transistor-Based Biosensor for Detection of Amyloid-Beta in Human Serum. *Biosens. Bioelectron.* 2013, 50, 345–350.
108. Kevadiya, B.D.; Machhi, J.; Herskovitz, J.; Oleynikov, M.D.; Blomberg, W.R.; Bajwa, N.; Soni, D.; Das, S.; Hasan, M.; Patel, M.; et al. Diagnostics for SARS-CoV-2 Infections. *Nat. Mater.* 2021, 20, 593–605.
109. Ferretti, L.; Wymant, C.; Kendall, M.; Zhao, L.; Nurtay, A.; Abeler-Dörner, L.; Parker, M.; Bonsall, D.; Fraser, C. Quantifying SARS-CoV-2 Transmission Suggests Epidemic Control with Digital Contact Tracing. *Science* 2020, 368, eabb6936.
110. Pinals, R.L.; Ledesma, F.; Yang, D.; Navarro, N.; Jeong, S.; Pak, J.E.; Kuo, L.; Chuang, Y.-C.; Cheng, Y.-W.; Sun, H.-Y.; et al. Rapid SARS-CoV-2 Spike Protein Detection by Carbon Nanotube-Based Near-Infrared Nanosensors. *Nano Lett.* 2021, 21, 2272–2280.
111. Yang, J.; Petitjean, S.J.L.; Koehler, M.; Zhang, Q.; Dumitru, A.C.; Chen, W.; Derclaye, S.; Vincent, S.P.; Soumillion, P.; Alsteens, D. Molecular Interaction and Inhibition of SARS-CoV-2 Binding to the ACE2 Receptor. *Nat. Commun.* 2020, 11, 4541.
112. Kai, H.; Kato, Y.; Toyosato, R.; Nishizawa, M. Fluid-Permeable Enzymatic Lactate Sensors for Micro-Volume Specimen. *Analyst* 2018, 143, 5545–5551.
113. Bhushan, P.; Umasankar, Y.; RoyChoudhury, S.; Hirt, P.A.; MacQuhaec, F.E.; Borda, L.J.; Lev-Tov, H.A.; Kirsner, R.S.; Bhansali, S. Biosensor for Monitoring Uric Acid in Wound and Its Proximity: A Potential Wound Diagnostic Tool. *J.*

114. Zappi, D.; Caminiti, R.; Ingo, G.M.; Sadun, C.; Tortolini, C.; Antonelli, M.L. Biologically Friendly Room Temperature Ionic Liquids and Nanomaterials for the Development of Innovative Enzymatic Biosensors. *Talanta* 2017, 175, 566–572.
115. Chen, C.; Ran, R.; Yang, Z.; Lv, R.; Shen, W.; Kang, F.; Huang, Z.-H. An Efficient Flexible Electrochemical Glucose Sensor Based on Carbon Nanotubes/Carbonized Silk Fabrics Decorated with Pt Microspheres. *Sens. Actuators B Chem.* 2018, 256, 63–70.
116. Madhurantakam, S.; Jayanth Babu, K.; Balaguru Rayappan, J.B.; Krishnan, U.M. Fabrication of Mediator-Free Hybrid Nano-Interfaced Electrochemical Biosensor for Monitoring Cancer Cell Proliferation. *Biosens. Bioelectron.* 2017, 87, 832–841.
117. Singh, A.K.; Singh, M.; Verma, N. Electrochemical Preparation of Fe₃O₄/MWCNT-Polyaniline Nanocomposite Film for Development of Urea Biosensor and Its Application in Milk Sample. *J. Food Meas. Charact.* 2020, 14, 163–175.
118. Magar, H.S.; Ghica, M.E.; Abbas, M.N.; Brett, C.M.A. A Novel Sensitive Amperometric Choline Biosensor Based on Multiwalled Carbon Nanotubes and Gold Nanoparticles. *Talanta* 2017, 167, 462–469.
119. Alizadeh, T.; Nayeri, S. An Enzyme-Free Sensing Platform Based on Molecularly Imprinted Polymer/MWCNT Composite for Sub-Micromolar-Level Determination of Pyruvic Acid as a Cancer Biomarker. *Anal. Bioanal. Chem.* 2020, 412, 657–667.
120. Arkan, E.; Saber, R.; Karimi, Z.; Shamsipur, M. A Novel Antibody–Antigen Based Impedimetric Immunosensor for Low Level Detection of HER2 in Serum Samples of Breast Cancer Patients via Modification of a Gold Nanoparticles Decorated Multiwall Carbon Nanotube-Ionic Liquid Electrode. *Anal. Chim. Acta* 2015, 874, 66–74.
121. Nawaz, M.A.H.; Majdinasab, M.; Latif, U.; Nasir, M.; Gokce, G.; Anwar, M.W.; Hayat, A. Development of a Disposable Electrochemical Sensor for Detection of Cholesterol Using Differential Pulse Voltammetry. *J. Pharm. Biomed. Anal.* 2018, 159, 398–405.
122. Jeong, H.; Nguyen, D.M.; Lee, M.S.; Kim, H.G.; Ko, S.C.; Kwac, L.K. N-Doped Graphene-Carbon Nanotube Hybrid Networks Attaching with Gold Nanoparticles for Glucose Non-Enzymatic Sensor. *Mater. Sci. Eng. C* 2018, 90, 38–45.
123. Riberi, W.I.; Tarditto, L.V.; Zon, M.A.; Arévalo, F.J.; Fernández, H. Development of an Electrochemical Immunosensor to Determine Zearalenone in Maize Using Carbon Screen Printed Electrodes Modified with Multi-Walled Carbon Nanotubes/Polyethyleneimine Dispersions. *Sens. Actuators B Chem.* 2018, 254, 1271–1277.
124. Chen, M.; Wu, D.; Tu, S.; Yang, C.; Chen, D.; Xu, Y. A Novel Biosensor for the Ultrasensitive Detection of the LncRNA Biomarker MALAT1 in Non-Small Cell Lung Cancer. *Sci. Rep.* 2021, 11, 3666.
125. Sabahi, A.; Salahandish, R.; Ghaffarinejad, A.; Omidinia, E. Electrochemical Nano-Genosensor for Highly Sensitive Detection of MiR-21 Biomarker Based on SWCNT-Grafted Dendritic Au Nanostructure for Early Detection of Prostate Cancer. *Talanta* 2020, 209, 120595.
126. Rostamabadi, P.F.; Heydari-Bafrooei, E. Impedimetric Aptasensing of the Breast Cancer Biomarker HER2 Using a Glassy Carbon Electrode Modified with Gold Nanoparticles in a Composite Consisting of Electrochemically Reduced Graphene Oxide and Single-Walled Carbon Nanotubes. *Microchim. Acta* 2019, 186, 495.
127. Phonklam, K.; Wannapob, R.; Sriwimol, W.; Thavarungkul, P.; Phairatana, T. A Novel Molecularly Imprinted Polymer PMB/MWCNTs Sensor for Highly-Sensitive Cardiac Troponin T Detection. *Sens. Actuators B Chem.* 2020, 308, 127630.
128. Kumar, T.H.V.; Sundramoorthy, A.K. Non-Enzymatic Electrochemical Detection of Urea on Silver Nanoparticles Anchored Nitrogen-Doped Single-Walled Carbon Nanotube Modified Electrode. *J. Electrochem. Soc.* 2018, 165, B3006–B3016.
129. Qian, Q.; Hu, Q.; Li, L.; Shi, P.; Zhou, J.; Kong, J.; Zhang, X.; Sun, G.; Huang, W. Sensitive Fiber Microelectrode Made of Nickel Hydroxide Nanosheets Embedded in Highly-Aligned Carbon Nanotube Scaffold for Nonenzymatic Glucose Determination. *Sens. Actuators B Chem.* 2018, 257, 23–28.
130. Palve, Y.P.; Jha, N. A Novel Bilayer of Copper Nanowire and Carbon Nanotube Electrode for Highly Sensitive Enzyme Free Glucose Detection. *Mater. Chem. Phys.* 2020, 240, 122086.
131. Tan, C.; Dutta, G.; Yin, H.; Siddiqui, S.; Arumugam, P.U. Detection of Neurochemicals with Enhanced Sensitivity and Selectivity via Hybrid Multiwall Carbon Nanotube-Ultrananocrystalline Diamond Microelectrodes. *Sens. Actuators B Chem.* 2018, 258, 193–203.
132. Zhang, S.; Zahed, M.A.; Sharifuzzaman, M.; Yoon, S.; Hui, X.; Chandra Barman, S.; Sharma, S.; Yoon, H.S.; Park, C.; Park, J.Y. A Wearable Battery-Free Wireless and Skin-Interfaced Microfluidics Integrated Electrochemical Sensing Patch for on-Site Biomarkers Monitoring in Human Perspiration. *Biosens. Bioelectron.* 2021, 175, 112844.

133. Safaee, M.M.; Gravely, M.; Roxbury, D. A Wearable Optical Microfibrous Biomaterial with Encapsulated Nanosensors Enables Wireless Monitoring of Oxidative Stress. *Adv. Funct. Mater.* 2021, 31, 2006254.
134. Ma, H.; Xue, N.; Li, Z.; Xing, K.; Miao, X. Ultrasensitive Detection of MiRNA-155 Using Multi-Walled Carbon Nanotube-Gold Nanocomposites as a Novel Fluorescence Quenching Platform. *Sens. Actuators B Chem.* 2018, 266, 221–227.
135. Elmizadeh, H.; Faridbod, F.; Soleimani, M.; Ganjali, M.R.; Bardajee, G.R. Fluorescent Apt-Nanobiosensors for Fast and Sensitive Detection of Digoxin in Biological Fluids Using RGQDs: Comparison of Two Approaches for Immobilization of Aptamer. *Sens. Actuators B Chem.* 2020, 302, 127133.
136. Ghrera, A.S.; Pandey, C.M.; Malhotra, B.D. Multiwalled Carbon Nanotube Modified Microfluidic-Based Biosensor Chip for Nucleic Acid Detection. *Sens. Actuators B Chem.* 2018, 266, 329–336.
137. Nandeshwar, R.; Tallur, S. Integrated Low Cost Optical Biosensor for High Resolution Sensing of Myeloperoxidase (MPO) Activity Through Carbon Nanotube Degradation. *IEEE Sens. J.* 2021, 21, 1236–1243.
138. Shao, W.; Shurin, M.R.; Wheeler, S.E.; He, X.; Star, A. Rapid Detection of SARS-CoV-2 Antigens Using High-Purity Semiconducting Single-Walled Carbon Nanotube-Based Field-Effect Transistors. *ACS Appl. Mater. Interfaces* 2021, 13, 10321–10327.
139. Alfaifi, S.Y.M.; Hussain, M.M.; Asiri, A.M.; Rahman, M.M. Glassy Carbon Electrodes Decorated with HgO/CNT Nanocomposite and Modified with a Conducting Polymer Matrix for Enzyme-Free Ascorbic Acid Detection. *ChemistrySelect* 2022, 7, e202200086.
140. Lee, J.; Adegoke, O.; Park, E.Y. High-Performance Biosensing Systems Based on Various Nanomaterials as Signal Transducers. *Biotechnol. J.* 2019, 14, 1800249.
141. Lee, J.; Takemura, K.; Park, E. Plasmonic Nanomaterial-Based Optical Biosensing Platforms for Virus Detection. *Sensors* 2017, 17, 2332.
142. Lee, J.; Morita, M.; Takemura, K.; Park, E.Y. A Multi-Functional Gold/Iron-Oxide Nanoparticle-CNT Hybrid Nanomaterial as Virus DNA Sensing Platform. *Biosens. Bioelectron.* 2018, 102, 425–431.
143. Lee, J.; Ahmed, S.R.; Oh, S.; Kim, J.; Suzuki, T.; Parmar, K.; Park, S.S.; Lee, J.; Park, E.Y. A Plasmon-Assisted Fluoro-Immunoassay Using Gold Nanoparticle-Decorated Carbon Nanotubes for Monitoring the Influenza Virus. *Biosens. Bioelectron.* 2015, 64, 311–317.
144. Wasik, D.; Mulchandani, A.; Yates, M.V. A Heparin-Functionalized Carbon Nanotube-Based Affinity Biosensor for Dengue Virus. *Biosens. Bioelectron.* 2017, 91, 811–816.
145. Zhang, X.; Lu, W.; Han, E.; Wang, S.; Shen, J. Hybrid Nanostructure-Based Immunosensing for Electrochemical Assay of Escherichia Coli as Indicator Bacteria Relevant to the Recycling of Urban Sludge. *Electrochim. Acta* 2014, 141, 384–390.
146. Li, T.; Zhu, F.; Guo, W.; Gu, H.; Zhao, J.; Yan, M.; Liu, S. Selective Capture and Rapid Identification of E. Coli O157:H7 by Carbon Nanotube Multilayer Biosensors and Microfluidic Chip-Based LAMP. *RSC Adv.* 2017, 7, 30446–30452.
147. Zhang, X.; Shen, J.; Ma, H.; Jiang, Y.; Huang, C.; Han, E.; Yao, B.; He, Y. Optimized Dendrimer-Encapsulated Gold Nanoparticles and Enhanced Carbon Nanotube Nanoprobes for Amplified Electrochemical Immunoassay of E. coli in Dairy Product Based on Enzymatically Induced Deposition of Polyaniline. *Biosens. Bioelectron.* 2016, 80, 666–673.
148. He, Z.; Cai, Y.; Yang, Z.; Li, P.; Lei, H.; Liu, W.; Liu, Y. A Dual-Signal Readout Enzyme-Free Immunosensor Based on Hybridization Chain Reaction-Assisted Formation of Copper Nanoparticles for the Detection of Microcystin-LR. *Biosens. Bioelectron.* 2019, 126, 151–159.
149. Han, C.; Doepke, A.; Cho, W.; Likodimos, V.; de la Cruz, A.A.; Back, T.; Heineman, W.R.; Halsall, H.B.; Shanov, V.N.; Schulz, M.J.; et al. A Multiwalled-Carbon-Nanotube-Based Biosensor for Monitoring Microcystin-LR in Sources of Drinking Water Supplies. *Adv. Funct. Mater.* 2013, 23, 1807–1816.
150. Queirós, R.B.; Noronha, J.P.; Marques, P.V.S.; Sales, M.G.F. Label-Free Detection of Microcystin-LR in Waters Using Real-Time Potentiometric Biosensors Based on Single-Walled Carbon Nanotubes Imprinted Polymers. *Procedia Eng.* 2012, 47, 758–761.
151. Viswanathan, S.; Wu, L.; Huang, M.-R.; Ho, J.A. Electrochemical Immunosensor for Cholera Toxin Using Liposomes and Poly(3,4-Ethylenedioxythiophene)-Coated Carbon Nanotubes. *Anal. Chem.* 2006, 78, 1115–1121.
152. Palomar, Q.; Gondran, C.; Holzinger, M.; Marks, R.; Cosnier, S. Controlled Carbon Nanotube Layers for Impedimetric Immunosensors: High Performance Label Free Detection and Quantification of Anti-Cholera Toxin Antibody. *Biosens. Bioelectron.* 2017, 97, 177–183.
153. Shahriar, S.; Mondal, J.; Hasan, M.; Revuri, V.; Lee, D.; Lee, Y.-K. Electrospinning Nanofibers for Therapeutics Delivery. *Nanomaterials* 2019, 9, 532.

154. Mondal, J.; Revuri, V.; Choochana, P.; Ganesan, P.; Kang, W.J.; Lee, Y. Sulfur and Nitrogen Doped Carbon Quantum Dots for Detection of Glutathione and Reduction of Cellular Nitric Oxide in Microglial Cells. *J. Pharm. Investig.* 2020, 50, 209–218.
-

Retrieved from <https://encyclopedia.pub/entry/history/show/66948>